A Deterministic-Solution Based Fast Eigenvalue Solver With Guaranteed Convergence for Finite-Element Based 3-D Electromagnetic Analysis

Feng Sheng and Dan Jiao, *Senior Member, IEEE*

***Abstract*—A fast solution to both the quadratic eigenvalue problem and the generalized eigenvalue problem is developed for the finite-element based analysis of general 3-D electromagnetic problems. Given an arbitrary frequency band of interest, denoting the number of physically important eigenvalues for this band by k, the proposed eigenvalue solution is capable of solving a significantly reduced eigenvalue problem of $O(k)$ to find a complete set of eigenvalues and eigenvectors that are physically important for the given frequency band. In addition to bypassing the need of solving a large-scale eigenvalue problem of $O(N)$, with N being the system matrix size, the reduced eigenvalue problem is constructed from $O(k)$ solutions to a deterministic problem. As a result, the methods that have been developed to solve deterministic problems and their fast solvers can all be readily leveraged to solve eigenvalue problems. Moreover, the proposed fast eigenvalue solution has guaranteed convergence and controlled accuracy, which is theoretically proved in this paper. The solution is applicable to general 3-D problems where the structures are arbitrary, materials are inhomogeneous, and both dielectrics and conductors can be lossy. Applications to microwave devices, package structures, and on-chip integrated circuits have demonstrated the accuracy, efficiency, and convergence of the proposed fast eigenvalue solution.**

***Index Terms*—Deterministic solutions, eigenvalue solutions, electromagnetic analysis, fast solvers, finite element methods, generalized eigenvalue problems, quadratic eigenvalue problems.**

I. Introduction

THE solution to eigenvalue problems is of great importance to electromagnetic analysis. This is not only because of the analysis of classical source-free problems such as waveguides, cavities, filters, and resonators, but also because of the analysis of general problems with sources. As shown in [1]–[4], the solution of a deterministic problem with a source can be rigorously found by solving a generalized eigenvalue problem that is formulated without a source. For example, in a lossless system, the solution to the frequency-domain finite-element system matrix at an arbitrary frequency is the superposition of the eigenvectors of a frequency-independent generalized eigenvalue problem [3]. The weight of each eigenvector in the field solution is determined by its corresponding eigenvalue, the frequency being simulated, and the projection of the right hand side vector (source) onto the eigenvector. The same is true for electromagnetic problems with lossy materials such as nonideal conductors and lossy dielectrics, in which the underlying eigenvalue problem is a quadratic eigenvalue problem [4], [9]. The fact that the solution to a deterministic problem is embedded in the eigenvalue solution to a source-free problem is similar to the fact that the matrix inverse has nothing do with right hand sides; however, from the inverse of a matrix, one can obtain the matrix solution for any right hand side. In current mainstream methods for solving electromagnetic problems, a system of equations is required to be solved over and over again for each right hand side as well as each frequency. In contrast, if a fast eigenvalue solution can be developed, then there is no need to repeat the solution for a different right hand side. Moreover, there is no need to repeat the solution for a different frequency either, as can be seen from [4].

However, to accentuate the aforementioned advantages of an eigenvalue solution for electromagnetic analysis, one has to first overcome the high computational cost associated with traditional eigenvalue solvers. For solving a generalized eigenvalue problem $\mathbf{A}x = \lambda \mathbf{B}x$ of size N, the computational complexity of traditional eigenvalue solvers such as the QR algorithm is $O(N^3)$ [5] since $\mathbf{B}^{-1}\mathbf{A}$ is generally dense. With state-of-the-art Arnoldi algorithms [5], [6], k eigenpairs of a generalized eigenvalue problem can be found in k steps of an Arnoldi iteration. The computational cost of each Arnoldi iteration step for solving a generalized eigenvalue problem, which is the cost of multiplying $\mathbf{B}^{-1}\mathbf{A}$ by a vector, has also been reduced to $O(N)$ by advanced algorithms in [7] and [8] for a 2.5-D finite-element based analysis of on-chip interconnect structures, and in [9] for a 3-D finite-element based analysis of general integrated circuit problems. However, there still exist a few bottleneck problems in an Arnoldi algorithm based eigenvalue solution of electromagnetic problems. First, the Arnoldi process typically converges first to the largest eigenvalues of the numerical system. However, it is not clear which k eigenvalues of the original eigenvalue problem will be found in k Arnoldi steps. To obtain k eigenvalues of physical importance, one may have to use $100k$ or $1000k$ Arnoldi steps rather than k steps, resulting in $100k$ or $1000k$ krylov-subspace vectors, which is not computationally efficient. Second, there is no systematic way to control the convergence of an Arnoldi iteration. In other words, it is not known

Manuscript received March 01, 2012; revised December 22, 2012; accepted April 06, 2013. Date of publication April 16, 2013; date of current version July 01, 2013. This work was supported by a Grant from Office of Naval Research under Award N00014-10-1-0482, and a Grant from the NSF under Awards 0747578 and 1065318.

The authors are with the School of Electrical and Computer Engineering, Purdue University, West Lafayette, IN 47907 USA (e-mail: fsheng@purdue.edu; djiao@purdue.edu).

Color versions of one or more of the figures in this paper are available online at http://ieeexplore.ieee.org.

Digital Object Identifier 10.1109/TAP.2013.2258315

at which step to stop the Arnoldi process. For example, if one stops at the *100*th step, it is still possible that at the *101*th step, a new eigenvalue that is physically important for a given frequency band appears. In mathematical literature, there has been a continued effort to improve the convergence and efficiency of the Arnoldi algorithm for large-scale eigenvalue problems [10]–[12].

The key contribution of this paper is a fast eigenvalue solver that overcomes the aforementioned shortcomings of an Arnoldi algorithm based eigenvalue solution for finite-element based analysis of general 3-D electromagnetic problems. Given an arbitrary frequency band of interest, the eigenvalues and eigenvectors obtained from the proposed eigenvalue solver are a complete set of physically important eigenvalues and eigenvectors for the given frequency band. No initial guess of eigenvalues is required. The physically important eigenvectors in this paper are defined as the eigenvectors that are important for the field solution in the given frequency band based on prescribed accuracy, and their corresponding eigenvalues are called physically important eigenvalues. Furthermore, the eigen-solutions are efficiently obtained by the proposed method from a reduced eigenvalue problem of $O(k)$, where k is the number of physically important eigenvalues. Moreover, the convergence of the proposed eigenvalue solvers is guaranteed, which is theoretically proved in this paper. In addition to bypassing the need for solving a large-scale eigenvalue problem of $O(N)$, the reduced eigenvalue problem of $O(k)$ is obtained from $O(k)$ solutions to a deterministic problem. As a result, the methods that have been developed to solve deterministic problems and their fast solvers can all be leveraged to find the solution of eigenvalue problems. The proposed fast eigenvalue solution is applicable to both quadratic eigenvalue problems arising from the finite-element based analysis of lossy problems and the generalized eigenvalue problem resulting from the analysis of lossless problems. The structures that can be simulated by the proposed method are arbitrary 3-D structures and the materials are inhomogeneous.

Different from the eigenvalue solvers developed in mathematical literature [10]–[12], the proposed eigenvalue solver utilizes the relationship between the solution of a frequency-domain finite-element based deterministic problem and that of an eigenvalue problem to identify the eigenvalues and eigenvectors that are physically important for a given frequency band. Moreover, the proposed eigenvalue solver reduces the original large-scale eigenvalue problem to a small eigenvalue problem by $O(k)$ deterministic solutions. Different from the model order reduction methods developed to solve deterministic problems, $\mathbf{A}x = b$, in electromagnetics such as [13]–[15], the proposed method solves generalized eigenvalue problems $\mathbf{A}x = \lambda \mathbf{B}x$ and quadratic eigenvalue problems $\lambda^2 \mathbf{A}x + \lambda \mathbf{B}x + \mathbf{C}x = 0$, where $\mathbf{A}$, $\mathbf{B}$, and $\mathbf{C}$ are sparse matrices, λ denotes an eigenvalue, and x is an eigenvector.

In the following Section II, we provide a background of the proposed work. In Section III, we present the proposed fast eigenvalue solver for solving the generalized eigenvalue problem associated with lossless problems. A theoretical proof on its accuracy and guaranteed convergence is also provided. In Section IV, we describe the proposed fast eigenvalue solver for solving the quadratic eigenvalue problem arising from the analysis of lossy problems, in which both dielectrics and conductors could be lossy. The performance of the proposed fast eigenvalue solvers is demonstrated by a number of numerical examples in Section V. Section VI relates to our conclusions.

II. Background

In 3-D electromagnetic problems, the electric field $\mathbf{E}$ satisfies the second-order vector wave equation

$$\nabla \times [{\mu_r}^{-1} \nabla \times \mathbf{E}] - k_0^2 \varepsilon_r \mathbf{E} + j\omega\mu_0\sigma\mathbf{E} = -jk_0 Z_0 \mathbf{J} \quad \text{in } V \quad (1)$$

subject to certain boundary conditions, where μ_0 is free-space permeability, μ_r is relative permeability, ε_r is relative permittivity, σ is conductivity, k_0 is free-space wave number, Z_0 is free-space impedance, and $\mathbf{J}$ is current density. In (1), both dielectric and conductor loss can contribute to the term associated with conductivity σ. The conductor loss plays an important role in many electromagnetic applications. For example, in digital integrated circuits, conductors cannot be treated as perfect conductors because skin depth is comparable to the physical dimension of conductors at the circuit operating frequencies.

By setting the excitation to be zero, a finite-element based analysis of (1) subject to its boundary conditions results in the following quadratic eigenvalue problem [4], [9]

$$\left(\lambda^2 \mathbf{T} + \lambda \mathbf{R} + \mathbf{S}\right) v = 0 \quad (2)$$

in which the eigenvalues λ correspond to complex resonant frequencies, and the eigenvectors v characterize the field distribution of each resonant mode. The relationship between complex resonance frequency f_r and λ is

$$f_r = \frac{\lambda}{2\pi j}. \quad (3)$$

The $\mathbf{S}$, $\mathbf{T}$, and $\mathbf{R}$ in (2) are all sparse matrices. They are assembled from their elemental contributions as the following:

$$\begin{aligned} \mathbf{T}^e &= \mu_0 \varepsilon \langle \mathbf{N}_i, \mathbf{N}_j \rangle_V \\ \mathbf{R}^e &= \mu_0 \sigma \langle \mathbf{N}_i, \mathbf{N}_j \rangle_V + \sqrt{\mu_0 \varepsilon_0} \langle \hat{n} \times \mathbf{N}_i, \hat{n} \times \mathbf{N}_j \rangle_{S_o} \\ \mathbf{S}^e &= \mu_r^{-1} \langle \nabla \times \mathbf{N}_i, \nabla \times \mathbf{N}_j \rangle_V \end{aligned} \quad (4)$$

where $\mathbf{N}$ denotes the edge basis function used to expand the unknown electric field $\mathbf{E}$ in each element, $\langle ., . \rangle_V$ denotes a volume integration in the 3-D computational domain V, and $\langle ., . \rangle_{S_o}$ represents a surface integral on the outermost boundary S_o. In (4), a first-order absorbing boundary condition is used. If Diritchlet- or Neumann-type boundary conditions are used, the second term of $\mathbf{R}$ shown in (4) does not exist. The $\mathbf{T}$ is called mass matrix, and $\mathbf{S}$ is called stiffness matrix. Since $\mathbf{T}$ is Hermitian positive definite, $\mathbf{S}$ and $\mathbf{R}$ are Hermitian positive semidefinite, the eigenvalues of (2) are real or come in complex conjugate pairs [16]. Moreover, the real part of the eigenvalues is no greater than zero [16], and hence the system is stable.

In a lossless system where $\mathbf{R}$ does not exist, (2) reverts to a generalized eigenvalue problem as the following:

$$\mathbf{S}v = \xi \mathbf{T}v. \quad (5)$$

Since $\mathbf{S}$ is semipositive definite and $\mathbf{T}$ is positive definite, the eigenvalues of (5) are nonnegative real numbers. Different from that in lossy problems, the resonance frequency is real. Its relationship with the eigenvalues of (5) is as the following:

$$f_r = \frac{\sqrt{\xi}}{2\pi}.$$

The application of (2) and (5) is not just limited to finding the resonance frequencies and resonance modes of a 3-D problem. The intrinsic property of a 3-D system has nothing to do with excitations. The solution of eigenvalue problems like (2) and (5), in fact, carries the intrinsic property of the system. With the solution of eigenvalue problems known, the response of the system to any possible excitation is also known. Therefore, having an efficient solution of eigenvalue problems also provides an alternative way of solving deterministic problems.

Despite the importance of the eigenvalue problems, the solution to the eigenvalue problems is, in general, computationally expensive. In next two sections, we present the proposed fast eigenvalue solvers.

III. Proposed Fast Generalized Eigenvalue Solver for Lossless Problems

This section includes the proposed fast eigenvalue solution for analyzing lossless problems, a theoretical proof on its accuracy and guaranteed convergence, and a discussion on the choice of simulation parameters.

A. Proposed Fast Eigenvalue Solution

As shown in Section II, the eigenvalue problem for the finite-element based analysis of a lossless problem can be written as a frequency-independent generalized eigenvalue problem

$$\mathbf{S}v = \xi \mathbf{T}v. \tag{6}$$

Given a frequency band of interest $[\omega_{\min}, \omega_{\max}]$, to obtain a complete set of eigenvalues and eigenvectors of (6) that are physically important for the given frequency band, we propose to first solve the following deterministic problem at a few frequencies within this band:

$$(-\omega^2\mathbf{T} + \mathbf{S})x = -j\omega b \tag{7}$$

where b is a right hand side vector. If the source used to excite the electromagnetic structure of interest is known, then, this source can be used as b to reveal the characteristics of the structure for the given excitation. For cases where the source is unknown, a detailed discussion on the choice of b is given in the following Section III-C.

After calculating the solution of (7), we store the field solution vectors in matrix $\mathbf{X}$ as the following:

$$\mathbf{X} = [x(\omega_1), x(\omega_2), x(\omega_3), \ldots] \tag{8}$$

where ω_i $(i = 1, 2, \ldots)$ are the angular frequencies selected from the given frequency band, and $x(\omega_i)$ $(i = 1, 2, \ldots)$ are the field solution vectors obtained at these frequencies. Given a frequency band $[\omega_{\min}, \omega_{\max}]$, we use a bisection method to choose frequencies. The first frequency ω_1 is chosen as $\omega_{\min}$, then $\omega_2 = \omega_{\max}$, $\omega_3 = (\omega_1 + \omega_2)/2$, $\omega_4 = (\omega_1 + \omega_3)/2$, $\omega_5 = (\omega_3 + \omega_2)/2$, and continue. The dimension of $\mathbf{X}$ is N by p, where N is the total number of unknowns, p is the number of frequency points simulated, which we increase until the convergence is reached. We develop the following method to determine the convergence.

With $\mathbf{X}$, we transform the original large-scale system matrix shown in (7) to a reduced matrix of size p, as shown in the following:

$$(\mathbf{A}_r)_{p\times p} = \mathbf{X}^T(-\omega^2\mathbf{T} + \mathbf{S})\mathbf{X}. \tag{9}$$

We then check the rank of (9) by performing a singular value decomposition (SVD) [5]. Since the matrix shown in (9) is a small matrix of size p, the cost of SVD is negligible. Given an accuracy requirement $\varepsilon_{\mathrm{SVD}}$, we determine the rank by counting the number of singular values of (9) that satisfy the following condition:

$$s_i \geq \mathrm{s}_{\max} \times \varepsilon_{\mathrm{SVD}} \tag{10}$$

where s_i denotes a singular value, and $s_{\max}$ is the maximum singular value. We keep increasing the number of frequency points simulated, p, until the rank of (9) does not change any more (the convergence will be proved in next subsection). In other words, once the rank of (9) saturates, we stop adding more solution vectors into $\mathbf{X}$. Assuming at this point, the number of frequency points that have been simulated is m, the $\mathbf{X}$ obtained is an N by m matrix. The reduced matrix $\mathbf{A}_r$ in (9) is symmetric and of size m. Its singular value decomposition can be written as

$$(\mathbf{A}_r)_{m\times m} = \mathbf{U}_{m\times k}\Sigma_{k\times k}{\mathbf{U}_{m\times k}}^T + \varepsilon_{\mathrm{SVD}}\mathbf{A}_r \tag{11}$$

where k is the rank determined based on accuracy requirement $\varepsilon_{\mathrm{SVD}}$, which is no greater than m.

The procedure so far can be viewed as a multipoint-based model order reduction [15], but with a different approach proposed to control its convergence. This approach can also be used by existing model order reduction methods for solving deterministic problems to control convergence. Next, we show how to extract eigenvalues and eigenvectors of (6) from (8).

After the rank of (11) saturates, i.e., the convergence is reached, using $\mathbf{X}_{N\times m}$ in (8) and $\mathbf{U}_{m\times k}$ in (11), we transform the original large-scale eigenvalue problem of $O(N)$ shown in (6) to a significantly reduced eigenvalue problem of $O(k)$ as shown below

$$\mathbf{S}_r u = \lambda_r \mathbf{T}_r u \tag{12}$$

where

$$\mathbf{S}_r = (\mathbf{X}\mathbf{U})^T\mathbf{S}(\mathbf{X}\mathbf{U}), \mathbf{T}_r = (\mathbf{X}\mathbf{U})^T\mathbf{T}(\mathbf{X}\mathbf{U}). \tag{13}$$

Since the size of (12), k, is very small compared to N, (12) can be readily solved by a traditional eigenvalue solver with little cost.

After solving (12), we obtain a complete set of eigenvalues that are physically important for the given frequency band. The

eigenvectors of (6), v, can be recovered from the eigenvectors of (12), u, as the following:

$$v = \mathbf{X}_{N\times m}\mathbf{U}_{m\times k}u. \tag{14}$$

In next subsection, we provide a theoretical proof on the convergence and accuracy of the proposed eigenvalue solver.

B. Theoretical Proof on the Accuracy and Guaranteed Convergence of the Proposed Eigenvalue Solution

We will first prove why the proposed eigenvalue solution converges. In other words, given a prescribed accuracy, why the rank of (9) will saturate regardless of the increase of p. We then prove upon convergence, the eigenvalues of the significantly reduced eigenvalue problem (12) constitute a complete set of the eigenvalues of (6) that are physically important for the given frequency band, and the eigenvectors shown in (14) are the corresponding eigenvectors.

We begin the proof by revealing the content of $\mathbf{X}$ shown in (8). The $\mathbf{X}$ is obtained from the field solutions computed at the frequencies within the given frequency band. Each column vector of $\mathbf{X}$ is the solution of (7) at a frequency. Based on [3], the solution of (7) can be written as

$$x(\omega) = \mathbf{V}(\Lambda - \omega^2\mathbf{I})^{-1}\mathbf{V}^T(-j\omega b) \tag{15}$$

where $\mathbf{V}$ is the eigenvector matrix of (6), and Λ is the diagonal matrix composed of the eigenvalues of (6). It is clear that (15) is the superposition of all the eigenvectors of (6), and the weight of each eigenvector $\mathbf{V}_i$ in $x(\omega)$ is $(\lambda_i - \omega^2)^{-1}\mathbf{V}_i{}^T(-j\omega b)$. Clearly, given a frequency ω, not all of the eigenvectors make important contributions to the field solution. Only those eigenvectors that have a large weight are important, and hence should be kept in the field solution, while other eigenvectors can be discarded based on prescribed accuracy. As defined earlier, the eigenvectors that are important for the field solution based on prescribed accuracy are termed physically important eigenvectors in this paper, and their corresponding eigenvalues are called physically important eigenvalues. Given a frequency band of interest $[\omega_{\min}, \omega_{\max}]$, from (15), it can be seen that all the eigenvalues located within the given frequency band, i.e., the eigenvalues satisfying the following condition

$$\omega_{\min} \le \sqrt{\lambda_i} \le \omega_{\max} \tag{16}$$

should be counted as physically important eigenvalues for the given frequency band because the weights of their corresponding eigenvectors are large in the field solution. Besides this set of eigenvalues, the eigenvalues that are close to the given frequency band can be physically important also. Therefore, the eigenvalues that are physically important for a given frequency band include both the eigenvalues within the frequency band and the eigenvalues that are close to the frequency band.

From (15), it can also be understood why a bisection method is used in this paper to select frequencies to construct $\mathbf{X}$ in (8). This is because the solution obtained at any frequency is dominated by the eigenvalues closest to this frequency as can be seen from (15). Thus, with a bisection method, once the rank of (9) saturates, we have covered all the eigenvalues that are important for the given frequency band.

Given an accuracy requirement ε, assuming the number of physically important eigenvalues for the given frequency band is k, (15) can be written as

$$x(\omega) = \mathbf{V}_{N\times k}(\Lambda_{k\times k} - \omega^2\mathbf{I})^{-1}\mathbf{V}_{N\times k}{}^T(-j\omega b) + x(\omega)\times\varepsilon. \tag{17}$$

Each column vector of $\mathbf{X}$ has a form as that shown in (17). Therefore, $\mathbf{X}$ can be written as

$$\mathbf{X} = \mathbf{V}_{N\times k}\mathbf{Z}_{k\times p} + \varepsilon\mathbf{X} \tag{18}$$

where $\mathbf{Z}_{k\times p}$ denotes the union of the p vectors obtained at p frequencies, each of which is one $(\Lambda_{k\times k} - \omega^2\mathbf{I})^{-1}\mathbf{V}_{N\times k}{}^T(-j\omega b)$.

With $\mathbf{X}$ revealed as (18), (9) can be written as

$$(\mathbf{A}_r)_{p\times p} = \mathbf{Z}_{k\times p}{}^T\mathbf{V}_{N\times k}{}^T(-\omega^2\mathbf{T} + \mathbf{S})\mathbf{V}_{N\times k}\mathbf{Z}_{k\times p} + \varepsilon\mathbf{A}_r. \tag{19}$$

Since $\mathbf{V}$ of (6) satisfies $\mathbf{V}^T\mathbf{S}\mathbf{V} = \Lambda$, $\mathbf{V}^T\mathbf{T}\mathbf{V} = \mathbf{I}$ [3], we have

$$(\mathbf{A}_r)_{p\times p} = \mathbf{Z}_{k\times p}{}^T(-\omega^2\mathbf{I} + \Lambda)_{k\times k}\mathbf{Z}_{k\times p} + \varepsilon\mathbf{A}_r. \tag{20}$$

Clearly, once p is increased to a certain extent, the rank of (20), and hence (9), becomes k and remains to be k no matter how much p is increased further. In other words, the rank of (9) saturates. With the above, we prove the convergence of the proposed eigenvalue solution. In practice, once the rank of (9) does not increase with the increase of p, the convergence is reached.

When the convergence is reached, assuming at which $p = m$, we perform an SVD on (9), which is (20), we obtain

$$(\mathbf{A}_r)_{m\times m} = \mathbf{U}_{m\times k}\Sigma_{k\times k}\mathbf{U}_{m\times k}{}^T + \varepsilon\mathbf{A}_r. \tag{21}$$

It is worth mentioning that if the number of important eigenvalues in a frequency band happens to be very large, the SVD cost can be high. In this case, one can break the frequency band into multiple smaller frequency bands so that m for each subband is small, and then use the proposed method to find the physically important eigenvectors in each small subband. The union of the eigenvectors found in each subband makes a complete set of the eigenvectors for the entire frequency band.

Next we prove the eigenvalues of the reduced eigenvalue problem (12) are the eigenvalues of (6). Furthermore, they are the complete set of eigenvalues that are physically important for the given frequency band.

Using (18), with $p = m$, we obtain

$$\mathbf{X}\mathbf{U} \overset{\varepsilon}{=} \mathbf{V}_{N\times k}\mathbf{Z}_{k\times m}\mathbf{U}_{m\times k} = \mathbf{V}_{N\times k}\tilde{\mathbf{Z}}_{k\times k} \tag{22}$$

where the ε above "=" denotes the level of accuracy, and $\tilde{\mathbf{Z}}_{k\times k} = \mathbf{Z}_{k\times m}\mathbf{U}_{m\times k}$. The $\tilde{\mathbf{Z}}$ is a full-rank matrix because the rank of $\mathbf{X}\mathbf{U}$ is k. Substituting (22) into (13), we have

$$\begin{aligned}\mathbf{S}_r &= \mathbf{U}^T\mathbf{X}^T\mathbf{S}\mathbf{X}\mathbf{U} = \tilde{\mathbf{Z}}^T\mathbf{V}_{N\times k}{}^T\mathbf{S}\mathbf{V}_{N\times k}\tilde{\mathbf{Z}} = \tilde{\mathbf{Z}}^T\Lambda_{k\times k}\tilde{\mathbf{Z}}\\ \mathbf{T}_r &= \tilde{\mathbf{Z}}^T\mathbf{V}_{N\times k}{}^T\mathbf{T}\mathbf{V}_{N\times k}\tilde{\mathbf{Z}} = \tilde{\mathbf{Z}}^T\tilde{\mathbf{Z}}.\end{aligned} \tag{23}$$

Substituting (23) into (12), we obtain

$$\tilde{\mathbf{Z}}^T\Lambda_{k\times k}\tilde{\mathbf{Z}}u = \lambda_r\tilde{\mathbf{Z}}^T\tilde{\mathbf{Z}}u. \tag{24}$$

Since $\tilde{\mathbf{Z}}$ is a full-rank matrix that is invertible, we have

$$\Lambda_{k\times k}\tilde{\mathbf{Z}}u = \lambda_r\tilde{\mathbf{Z}}u \tag{25}$$

which can be further written as

$$\Lambda_{k\times k}y = \lambda_r y, \text{ where, } y = \tilde{\mathbf{Z}}u. \tag{26}$$

It is clear that the solution to the above eigenvalue problem is

$$\lambda_{r,i} = \lambda_i, y_i = \mathbf{I}_i, \quad i = 1, 2, \ldots k \tag{27}$$

where $\mathbf{I}_i$ is the ith column in an identity matrix. Therefore, we prove that the eigenvalues of (12), λ_r, are the k eigenvalues of (5). These k eigenvalues are also the complete set of physically important eigenvalues for the given frequency band as can be seen from (17).

Finally, we prove the eigenvectors shown in (14) are the eigenvectors of (6). Substituting (22) into (14), we have

$$v = \mathbf{X}_{N\times m}\mathbf{U}_{m\times k}u = \mathbf{V}_{N\times k}\tilde{\mathbf{Z}}_{k\times k}u. \tag{28}$$

Since $u = \tilde{\mathbf{Z}}^{-1}y = \tilde{\mathbf{Z}}^{-1}\mathbf{I}_i$ as can be seen from (26) and (27), we obtain

$$v = \mathbf{X}_{N\times m}\mathbf{U}_{m\times k}u = \mathbf{V}_{N\times k}\tilde{\mathbf{Z}}\tilde{\mathbf{Z}}^{-1}\mathbf{I}_i = \mathbf{V}_{N\times k}\mathbf{I}_i \tag{29}$$

which is nothing but one column vector of the union of the k eigenvectors of (6) that are physically important for the given frequency band.

From the aforementioned proof, it can also be seen that the accuracy of the proposed fast eigenvalue solution is controllable. In numerical implementations, one can choose $\varepsilon_{\mathrm{SVD}}$ shown in (10) to satisfy a prescribed accuracy.

C. Choice of Right Hand Side Vectors

In the proposed eigenvalue solution, we employ the solutions obtained for a deterministic problem shown in (7) to solve (6). In (7), a right hand side vector b is involved. The validity of the proposed eigenvalue solution is not affected by the choice of b. In other words, regardless of the choice of b, one can identify a subset of the eigenvalues of the given frequency band since $\mathbf{V}^T b$ is not zero. Some of the eigenvectors will be excited by b as long as b is nonzero. However, if the objective is to find a complete set of eigenvalues that are physically important for a given frequency band, b should be chosen appropriately. As can be seen from (15), if the projection of b onto an eigenvector is zero, this eigenvector would not appear in the field solution, and hence cannot be found by the proposed eigenvalue solution. There are two ways to solve this problem. One is to select b that has a nonzero projection onto every eigenvector. This is actually not a difficult task since each eigenvector of (6) represents an $\mathbf{E}$-field solution of Maxwell's equations in the given problem subject to boundary conditions at all the material interfaces. Even though we do not know the detailed field distribution of an eigenvector, we know the $\mathbf{E}$ field must satisfy boundary conditions. For example, on a conducting surface, $\mathbf{E}$ must be perpendicular to the conducting surface. Thus, we can select corresponding entries in b to be nonzero. Such a choice of b will have a nonzero projection on all the eigenvectors. In practice, for convenience, one can select a vector made of random numbers as the right hand side b. This is what we used in all the examples simulated in Section V. This is because the chance for an eigenvector to have a zero projection onto a vector of random numbers, i.e., making $\mathbf{V}_i^T b = (b^T\mathbf{V}_i)^T$ zero for b consisting of N random numbers, is almost zero if not exactly zero. The other way is to choose b as the excitation commonly used to excite the structure being simulated. In this case, the excitation of the problem is known, thus the eigenvectors of physical importance are also those eigenvectors that can be excited by the given excitation.

IV. Proposed Fast Quadratic Eigenvalue Solver for Lossy Problems

In this section, we present the proposed eigenvalue solution for analyzing lossy problems in which both dielectrics and conductors can be lossy.

A. Proposed Fast Eigenvalue Solution

As shown in Section II, the eigenvalue problem underlying a general lossy problem is a frequency-independent quadratic eigenvalue problem as shown below

$$\left(\lambda^2\mathbf{T} + \lambda\mathbf{R} + \mathbf{S}\right)v = 0. \tag{30}$$

To obtain the eigenvalues and eigenvectors of (30), we solve the following deterministic problem at a few frequencies within the given frequency band:

$$(-\omega^2\mathbf{T} + j\omega\mathbf{R} + \mathbf{S})x = -j\omega b. \tag{31}$$

The choice of right hand side b is the same as that for lossless cases described in Section III-C. We then store the solution vectors in $\mathbf{X}$ as shown in (8), the column dimension of which is the number of frequency points simulated, denoted by p. With $\mathbf{X}$, we transform the original large-scale system matrix shown in (31) to a reduced matrix of size p, as shown in the following:

$$(\mathbf{A}_r)_{p\times p} = \mathbf{X}^T(-\omega^2\mathbf{T} + j\omega\mathbf{R} + \mathbf{S})\mathbf{X}. \tag{32}$$

Similar to the lossless cases, we increase the column dimension of $\mathbf{X}$ by simulating more and more frequency points until the rank of (33) does not change any more (The proof of convergence will be provided in next subsection). Assuming at this point, the number of frequency points that have been simulated is m, the $\mathbf{X}$ obtained is an N by m matrix. The reduced matrix $\mathbf{A}_r$ in (32) is symmetric and of size m. Its singular value decomposition can be written as

$$(\mathbf{A}_r)_{m\times m} = \mathbf{U}_{m\times k}\Sigma_{k\times k}{\mathbf{U}_{m\times k}}^T + \varepsilon_{\mathrm{SVD}}\mathbf{A}_r \tag{33}$$

where k is the rank determined based on accuracy requirement $\varepsilon_{\mathrm{SVD}}$. With $\mathbf{X}$ and the singular vector matrix $\mathbf{U}$ obtained at the convergence, we transform (30) to a significantly reduced eigenvalue problem of size k

$$\left(\lambda_r^2\mathbf{T}_r + \lambda_r\mathbf{R}_r + \mathbf{S}_r\right)v_r = 0 \tag{34}$$

where the reduced matrices $\mathbf{T}_r$, $\mathbf{R}_r$, and $\mathbf{S}_r$ of dimension k are

$$\begin{aligned}\mathbf{S}_r &= (\mathbf{X}\mathbf{U})^T\mathbf{S}(\mathbf{X}\mathbf{U}),\\ \mathbf{T}_r &= (\mathbf{X}\mathbf{U})^T\mathbf{T}(\mathbf{X}\mathbf{U}), \mathbf{R}_r = (\mathbf{X}\mathbf{U})^T\mathbf{R}(\mathbf{X}\mathbf{U}).\end{aligned} \tag{35}$$

The quadratic eigenvalue problem shown in (34) can be solved by computing the roots of the determinant of the polynomial matrix

$$\mathbf{P}(\lambda_r) = \lambda_r^2 \mathbf{T}_r + \lambda_r \mathbf{R}_r + \mathbf{S}_r. \tag{36}$$

However, this approach is not favorable in terms of computational efficiency. We thus linearize the quadratic eigenvalue problem (34) to a generalized eigenvalue problem of twice the dimension as shown below

$$\begin{bmatrix} -\mathbf{S}_r & 0 \\ 0 & \mathbf{T}_r \end{bmatrix} \begin{Bmatrix} v_r \\ \lambda_r v_r \end{Bmatrix} = \lambda_r \begin{bmatrix} \mathbf{R}_r & \mathbf{T}_r \\ \mathbf{T}_r & 0 \end{bmatrix} \begin{Bmatrix} v_r \\ \lambda_r v_r \end{Bmatrix}. \tag{37}$$

Notice that such linearization does not involve any theoretical approximation because the solution of (37) is the same as that of (34).

The generalized eigenvalue problem (37) can be compactly written as

$$\mathbf{A}_r \tilde{v}_r = \lambda_r \mathbf{B}_r \tilde{v}_r \tag{38}$$

where

$$\mathbf{A}_r = \begin{bmatrix} -\mathbf{S}_r & 0 \\ 0 & \mathbf{T}_r \end{bmatrix}, \ \mathbf{B}_r = \begin{bmatrix} \mathbf{R}_r & \mathbf{T}_r \\ \mathbf{T}_r & 0 \end{bmatrix}, \quad \tilde{v}_r = \begin{pmatrix} v_r \\ \lambda_r v_r \end{pmatrix}. \tag{39}$$

The (38) is a significantly reduced eigenvalue problem of dimension $2k$, which can be readily solved.

From the solution of (38), we obtain a complete set of eigenvalues of (30) that are physically important for the given frequency band. The eigenvectors of (30), v, can be recovered from the eigenvector of (34), v_r, which is the upper half of the eigenvector of (38), as the following:

$$v = \mathbf{X}_{N\times m} \mathbf{U}_{m\times k} v_r. \tag{40}$$

In a lossy system where nonideal conductors are present, the matrix norm $\|\mathbf{T}\|_2$, $\|\mathbf{S}\|_2$, and $\|\mathbf{R}\|_2$ can differ by orders of magnitude. In this case, directly solving (38) may yield very poor errors [17], [18]. As a result, we have to scale the underlying matrices before solving (38) for achieving good accuracy. We employ an optimal scaling technique [17] to reduce the error of the eigenvalue solution. There are two scaling coefficients α and β involved in this technique. They are determined as the following:

$$\begin{aligned} &\gamma_2 = \|\mathbf{T}_r\|, \ \gamma_1 = \|\mathbf{R}_r\|, \ \gamma_0 = \|\mathbf{S}_r\| \\ &\alpha = \sqrt{\frac{\gamma_0}{\gamma_2}}, \\ &\beta = \frac{2}{(\gamma_0 + \gamma_1 \alpha)}. \end{aligned} \tag{41}$$

Based on the optimal scaling coefficients, we convert the original quadratic problem $\mathbf{P}$ shown in (36) to a scaled quadratic problem as the following:

$$\left(\lambda''^2 \alpha^2 \beta \mathbf{T}_r + \lambda'' \alpha \beta \mathbf{R}_r + \beta \mathbf{S}_r\right) v'' = 0. \tag{42}$$

After solving (42), the eigenpairs of the original quadratic eigenvalue problem (34) can be recovered from

$$\lambda_r = \alpha \lambda'', \ v_r = v''.$$

The error of a quadratic eigenvalue problem like (30) can be assessed by the backward error [17], [18] defined as the following:

$$\eta(\lambda, v) = \frac{\left\|(\lambda^2 \mathbf{T} + \lambda \mathbf{R} + \mathbf{S}) v\right\|_2}{\left(|\lambda|^2 \|\mathbf{T}\|_2 + |\lambda| \, \|\mathbf{R}\|_2 + \|\mathbf{S}\|_2\right) \|v\|_2}. \tag{43}$$

B. Theoretical Proof on the Accuracy and Guaranteed Convergence of the Proposed Eigenvalue Solution

To provide a theoretical proof of the proposed quadratic eigenvalue solution, similar to lossless cases, we first need to develop a theoretical understanding on $\mathbf{X}$. The $\mathbf{X}$ is obtained from the field solutions computed at the frequencies within the given frequency band. Each column vector of $\mathbf{X}$ is the solution of (31) simulated at a frequency. Based on [4], the solution of (31) can be written as

$$x(\omega) = \mathbf{V}_u (\Lambda + j\omega \mathbf{I})^{-1} (\mathbf{V}^T \mathbf{B} \mathbf{V})^{-1} \mathbf{V}_u{}^T (-j\omega b) \tag{44}$$

where $\mathbf{V}_u$ is the upper half of the eigenvector matrix $\mathbf{V}$, and Λ is the diagonal matrix composed of the eigenvalues of the following generalized eigenvalue problem:

$$\mathbf{A}\tilde{v} = \lambda \mathbf{B} \tilde{v} \tag{45}$$

where

$$\mathbf{A} = \begin{bmatrix} -\mathbf{S} & \\ & \mathbf{T} \end{bmatrix}, \ \mathbf{B} = \begin{bmatrix} \mathbf{R} & \mathbf{T} \\ \mathbf{T} & \end{bmatrix}, \ \tilde{v} = \begin{pmatrix} v \\ \lambda v \end{pmatrix}. \tag{46}$$

Similar to the fact that the solution of (38) is the same as that of (34), the solution of (45) is the same as that of (30).

It is clear that (44) is the superposition of all the eigenvectors of (45), and the weight of each eigenvector $\mathbf{V}_i$ in $x(\omega)$ is proportional to $(\lambda_i + j\omega)^{-1}$. Clearly, given a frequency ω, not all of the eigenvectors make important contributions to the field solution. Only those eigenvectors having a large weight are important in the field solution, and other eigenvectors can be truncated based on prescribed accuracy. Therefore, based on (44), similar to lossless cases, $\mathbf{X}$ can be written as

$$\mathbf{X} = (\mathbf{V}_u)_{N\times k} \mathbf{Z}_{k\times p} + \varepsilon \mathbf{X} \tag{47}$$

where k is the number of physically important eigenvectors that should be kept in the field solution based on accuracy requirement ε, and $\mathbf{Z}_{k\times p}$ denotes the union of the p vectors obtained at p frequencies, each of which is the term right multiplied with $\mathbf{V}_u$ in (44).

With $\mathbf{X}$ known in (47), (32) can be rewritten as

$$\begin{aligned} (\mathbf{A}_r)_{p\times p} = {} & \mathbf{Z}_{k\times p}{}^T (\mathbf{V}_u)_{N\times k}{}^T \\ & \times (-\omega^2 \mathbf{T} + j\omega \mathbf{R} + \mathbf{S}) (\mathbf{V}_u)_{N\times k} \mathbf{Z}_{k\times p} + \varepsilon \mathbf{A}_r \end{aligned} \tag{48}$$

which is a rank-k matrix when p is increased to be no less than k. After that, no matter how much p is increased, the rank of (48), and hence (32), remains the same. With the above, we prove the convergence of the proposed quadratic eigenvalue solution for simulating lossy problems.

Using (47), with $p = m$ when convergence is reached, we obtain

$$\mathbf{XU} \stackrel{\varepsilon}{=} (\mathbf{V}_u)_{N\times k}\mathbf{Z}_{k\times m}\mathbf{U}_{m\times k} = (\mathbf{V}_u)_{N\times k}\tilde{\mathbf{Z}}_{k\times k} \tag{49}$$

where $\tilde{\mathbf{Z}}_{k\times k} = \mathbf{Z}_{k\times m}\mathbf{U}_{m\times k}$ is a full-rank matrix. Substituting the above into (34), we obtain

$$\tilde{\mathbf{Z}}^T(\mathbf{V}_u)_{N\times k}{}^T\left(\lambda_r^2\mathbf{T} + \lambda_r\mathbf{R} + \mathbf{S}\right)(\mathbf{V}_u)_{N\times k}\tilde{\mathbf{Z}}v_r = 0. \tag{50}$$

Since $\tilde{\mathbf{Z}}$ is invertible, we have

$$(\mathbf{V}_u)_{N\times k}{}^T\left(\lambda_r^2\mathbf{T} + \lambda_r\mathbf{R} + \mathbf{S}\right)(\mathbf{V}_u)_{N\times k}\tilde{\mathbf{Z}}v_r = 0. \tag{51}$$

Since $(\lambda_i, \mathbf{V}_{u,i})$ is the eigenpair of (45), and hence the solution of (2), the solution to the above eigenvalue problem (51) is

$$\lambda_{r,i} = \lambda_i, \tilde{\mathbf{Z}}v_{r,i} = \mathbf{I}_i, \quad i = 1, 2, \ldots k. \tag{52}$$

Thus, we prove that the eigenvalues of the reduced eigenvalue problem (34) are the k physically important eigenvalues of the original eigenvalue problem (30).

Moreover, substituting (49) into (40), we have

$$v = \mathbf{X}_{N\times m}\mathbf{U}_{m\times k}v_r = (\mathbf{V}_u)_{N\times k}\tilde{\mathbf{Z}}_{k\times k}v_r. \tag{53}$$

Since $v_{r,i} = \tilde{\mathbf{Z}}^{-1}\mathbf{I}_i$ as can be seen from (52), we obtain

$$v = \mathbf{X}_{N\times m}\mathbf{U}_{m\times k}v_r = (\mathbf{V}_u)_{N\times k}\tilde{\mathbf{Z}}\tilde{\mathbf{Z}}^{-1}\mathbf{I}_i = (\mathbf{V}_u)_{N\times k}\mathbf{I}_i \tag{54}$$

which is nothing, but one column vector of the k physically important eigenvectors of (45), and hence (30). As a result, we prove that the eigenvectors obtained from (40) are the eigenvectors of the original eigenvalue problem (30) that are physically important for the given frequency band.

V. Numerical Results

A suite of examples from microwave cavities to on-chip interconnects was simulated to demonstrate the accuracy, efficiency, and convergence of the proposed eigenvalue solver. For all these examples, the right hand side vector is chosen as a vector of N random numbers. The bisection method is used to choose frequencies in the given frequency band until the proposed eigenvalue solver converges.

A. Rectangular Microwave Cavities

We first validated the proposed method with a set of microwave structures, the analytical resonant frequencies of which were given in [19].

The first microwave structure is a half-filled 1 cm $\times$ 0.1 cm $\times$ 1 cm rectangular cavity with a dielectric material of $\varepsilon_r = 2$ extending from $z = 0.5$ cm to $z = 1$ cm, as shown in Fig. 1. The left half of the cavity is filled by air. The rectangular cavity is shielded with perfect electric conductors (PEC) all around.

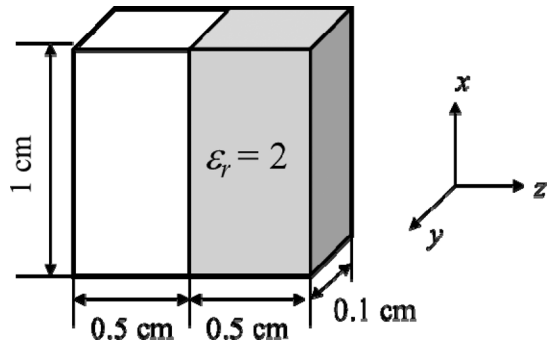

Fig. 1. Lossless half-filled rectangular cavity.

The finite element based discretization results in 1575 unknowns. The frequency band of interest is [1 GHz, 50 GHz]. The proposed eigenvalues solver is applied to find a complete set of eigenvalues that are physically important for the given frequency band. As mentioned before, this set of eigenvalues includes all the eigenvalues within the given frequency band and the eigenvalues that are close to the given frequency band. The SVD error used in (10), $\varepsilon_{\mathrm{SVD}}$, is chosen as 10^{-16}. Given such an accuracy criterion, the proposed eigenvalue solver converges when the column dimension of $\mathbf{X}$ reaches 20, i.e., m in (11) is 20. The resultant rank of (9), and hence (11), is 15, which saturates no matter how much the column dimension of $\mathbf{X}$ further grows. The dimension of the reduced eigenvalue problem (12), and hence the number of physically important eigenvalues, k, is 15, which agrees with the number obtained by directly solving the original eigenvalue problem (6). Compared to the size of the original eigenvalue problem (6), which is 1575, the reduction is significant. Moreover, the proposed eigenvalue solver is capable of producing a complete set of eigenvalues that are physically important for the given frequency band with guaranteed convergence and controlled accuracy. In Table I, we list the lowest four resonance wave numbers obtained from the proposed eigenvalue solver in comparison with analytical data. Excellent agreement is observed. In Table II, we compare both eigenvalues and eigenvectors of (6) generated by the proposed eigenvalue solver with those obtained from the eigenvalue solver in Matlab. Excellent agreement is observed in both eigenvalues and eigenvectors. The eigenvector relative error is defined as $\|v - v_{ref}\|/\|v_{ref}\|$, where v is computed from the proposed solver, and v_{ref} is the eigenvector generated from Matlab's eigenvalue solver. It is worth mentioning that Table I shows an error much larger than that given in Table II because the comparison is made with analytical solution, and the error contains the space discretization error. To improve the accuracy of Table I, one can refine the mesh. To verify, we double the mesh elements along both x and z directions, which results in 6745 unknowns. The errors of the four eigenvalues in Table I are shown to be 0.11%, 0.15%, 0.15%, and 0.17% respectively, and hence reduced. We also simulate the same example by using a lower-order accuracy setting of $\varepsilon_{\mathrm{SVD}} = 10^{-12}$. As expected,

TABLE I
RESONANT WAVE NUMBERS OF A LOSSLESS CAVITY

Mode	Analytical Data [cm^{-1}]	Proposed Solver [cm^{-1}]	Relative Error [%]
TEz_{101}	3.5378	3.5494	0.32
TEz_{102}	5.9979	6.0122	0.23
TEz_{202}	7.6331	7.7070	0.96
TEz_{103}	8.0957	8.1551	0.73

TABLE II
EIGENVALUE AND EIGENVECTOR ERRORS OF A LOSSLESS CAVITY

Mode	Eigenvalue	Eigenvalue Relative Error	Eigenvector Relative Error
TEz_{101}	1.1328×10^{22}	7.20×10^{-14}	1.34×10^{-9}
TEz_{102}	3.2502×10^{22}	4.07×10^{-13}	1.19×10^{-8}
TEz_{202}	5.3409×10^{22}	1.11×10^{-7}	3.07×10^{-4}
TEz_{103}	5.9800×10^{22}	1.95×10^{-9}	4.71×10^{-5}

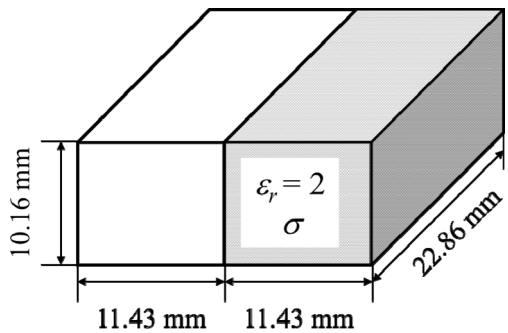

Fig. 2. Lossy half-filled rectangular cavity.

TABLE III
LOWEST RESONANT FREQUENCIES OF A LOSSY RECTANGULAR CAVITY

σ [S/m]	Analytical Data [GHz]	Proposed Solver [GHz]
0.1	7.379 + j0.354	7.398 + j0.354
0.5	7.236 + j1.819	7.256 + j1.814
1.0	6.579 + j3.864	6.605 + j3.853
1.3	5.711 + j5.197	5.749 + j5.183

TABLE IV
RESONANT FREQUENCIES OF A LOSSLESS 1 CM × 1 CM × 2 CM CAVITY

Mode	Analytical Data [GHz]	Proposed Solver [GHz]
0 1 1	16.771	16.7845
1 0 1	16.771	16.8222
1 1 0	21.213	21.2119
0 1 2	21.213	21.2356
1 0 2	21.213	21.6716
1 1 1	22.50	22.5002
1 1 2	25.98	26.0055

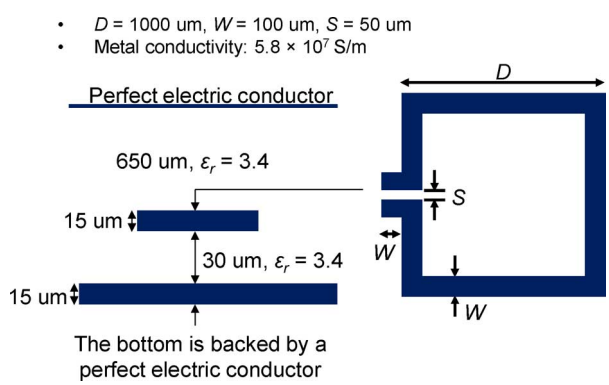

Fig. 3. Illustration of a package inductor.

the eigenvalues obtained are less accurate than those in Table I. The errors for the four eigenvalues are shown to be 0.32%, 0.25%, 1.35%, and 6.64%, respectively. The last eigenvalue appears to be affected the most in accuracy. This can be due to the fact that the singular values associated with this mode are affected the most by the new truncation criterion.

Next, we consider a rectangular resonator half filled by a conductive material, as shown in Fig. 2. The dimension of the resonator is 22.86 mm × 22.86 cm × 10.16 mm. The conductive material has relative permittivity $\varepsilon_r = 2$ and conductivity σ that ranges from 0.1 to 1.3. Again the rectangular cavity is shielded by perfect electric conductors.

The quadratic eigenvalue problem shown in (31) is solved by the proposed method. The frequency band of interest is [1 GHz, 50 GHz]. The SVD error used in (10), $\varepsilon_{\mathrm{SVD}}$, is chosen as 10^{-16}. In Table III, we list the lowest resonance frequencies obtained from the proposed eigenvalue solver in comparison with analytical data. Excellent agreement is observed. For simulating the four cases with $\sigma = 0.1$, 0.5, 1.0, and 1.3 S/m respectively, the column dimension of $\mathbf{X}$ upon convergence is 39, 37, 37, and 36 respectively. The number of physically important eigenvalues, k, in the given frequency band are found to be 36, 35, 35, and 34, respectively.

To assess the capability of the proposed eigenvalue solver in identifying degenerate eigenvalues, we simulated a PEC cavity of dimension 1 cm × 1 cm × 2 cm. The finite element based discretization results in 29, 260 unknowns. The frequency band considered is [10 GHz, 30 GHz]. The SVD error $\varepsilon_{\mathrm{SVD}}$ is chosen as 10^{-16}. Given such an accuracy criterion, the proposed eigenvalue solver converges when the column dimension of $\mathbf{X}$ reaches 19. The resultant rank of (9) is 15, which saturates no matter how much the column dimension of $\mathbf{X}$ further grows. In Table IV, we list the first seven resonant frequencies in the given frequency band obtained from the proposed eigenvalue solver in comparison with analytical data. Very good agreement is observed. It is also observed that although the degenerate eigenvalues analytically are identical, what is numerically found can have a slight difference.

B. Package Inductor

We simulated a package inductor example, the detailed geometry and material information of which are given in Fig. 3. In this example, we also compared the CPU time cost of the proposed eigenvalue solution with that of a state-of-the-art Arnoldi based sparse eigenvalue solver in Matlab.

A finite element based discretization results in 1499 unknowns. Since conductor loss is involved, the proposed method is used to solve a quadratic eigenvalue problem shown in (2) to find a complete set of eigenvalues and eigenvectors that are physically important for frequency band [1 GHz, 100 GHz]. The SVD error used in (10), $\varepsilon_{\mathrm{SVD}}$, is chosen as 1.0×10^{-12}. The proposed eigenvalue solver converges when $\mathbf{X}$ reaches

TABLE V
LOWEST FIVE RESONANCE FREQUENCIES OF A PACKAGE INDUCTOR

Direct Solver [GHz]	Proposed Solver [GHz]	Backward Error
22.393 + j0.026	22.393 + j0.026	3.815×10^{-13}
54.908 + j0.031	54.908 + j0.031	9.173×10^{-14}
68.512 + j0.000	68.513 + j0.000	2.009×10^{-12}
89.686 + j0.027	89.687 + j0.027	4.314×10^{-11}
101.73 + j0.001	101.75 + j0.001	1.470×10^{-9}

TABLE VI
STEPS AND CPU TIME FOR FINDING THE EIGENSOLUTION OF A PACKAGE INDUCTOR IN THE FREQUENCY BAND [1 GHz, 100 GHz]

Conventional Solver	Proposed Solver	
CPU Time [s]	Column Dimension of X	CPU Time [s]
43.7	15	0.86

a column dimension of 15. The rank of (33) saturates at 12, which is also the number of physically important eigenvalues, k, solved from (34).

In Table V, we compare the resonance frequencies generated by the proposed eigenvalue solver with those generated by Matlab. Excellent agreement can be observed. The backward error, shown in (43), of the proposed eigenvalue solver is also given in Table V. Good accuracy of the proposed solver can be clearly seen.

To evaluate the efficiency of the proposed method, we compare its performance with that of a state-of-the-art Arnoldi-based sparse eigenvalue solver provided by Matlab. When using the eigenvalue solver in Matlab, we use a central frequency $\mathrm{f}_0 = 55$ GHz to accelerate Matlab's eigenvalue solution to find the resonant frequencies in the range of [1 GHz, 100 GHz]. The Matlab's solver outputs one zero eigenvalue and the lowest five nonzero eigenvalues in six Arnoldi steps, the CPU cost of which is given in Table VI. We find that the Arnoldi-based eigenvalue solver in Matlab is sensitive to the choice of f_0. For example, if we choose $\mathrm{f}_0 = 50$ GHz, it can take more than 200 Arnoldi steps to find the first five nonzero resonant frequencies. Moreover, the Arnoldi-based eigenvalue solver cannot guarantee that all the important eigenvalues are found in a certain number of Arnoldi steps, i.e., there is no systematic way to control the convergence. Table VI compares the CPU time of the proposed eigenvalue solver with that cost by Matlab. It is shown that the proposed solver takes much less time than the Matlab's eigenvalue solver.

C. On-Chip Interconnect

The last example is an on-chip 3-D interconnect example shown in Fig. 4. The structure is of size 6 μm$\times$ 5 μm$\times$ 7 μm, with its upper and lower boundaries shielded by perfect electric conductors. Copper wires with conductivity $\sigma = 5 \times 10^7$ are orientated in x and y directions. The geometrical and material data are given in Fig. 4(a) and (b). The unit of the length, width, spacing, thickness shown in Fig. 4 is μm. The symbol Mi $(i = 1, 2, \ldots, 5)$ denotes the ith metal layer, and ε_r is relative permittivity.

The discretization results in 2314 unknowns. Due to the small feature size of the structure, its resonant frequencies are very

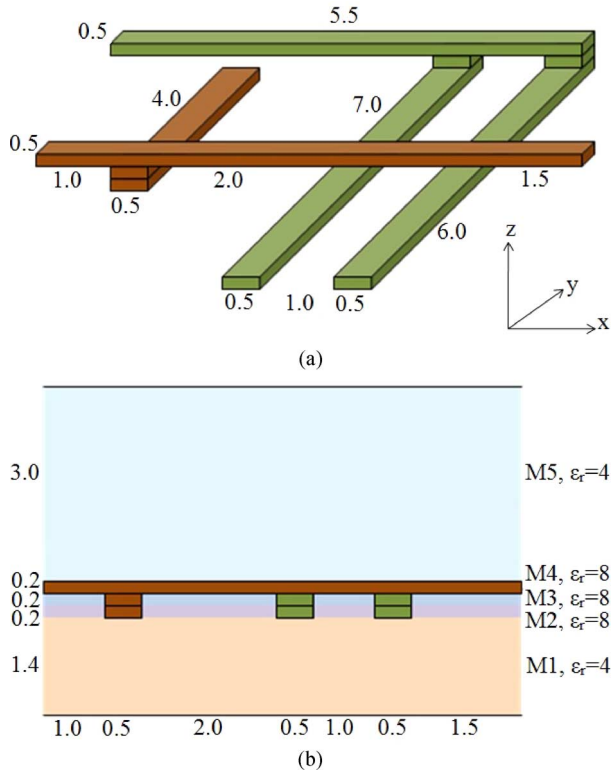

Fig. 4. Illustration of a lossy on-chip 3-D interconnect structure. (a) 3-D view of the structure. (b) xz-plane cross-sectional view.

TABLE VII
LOWEST THREE RESONANCE FREQUENCIES OF AN ON-CHIP INTERCONNECT

Resonance frequencies from Proposed Method [GHz]	Backward Error
2,403.7 + j53.4	4.048×10^{-10}
8,049.6 + j80.1	2.275×10^{-9}
9,933.6 + j52.1	6.998×10^{-9}

high. The frequency band computed is [1 kGHz, 10 kGHz]. The SVD error used in (10), $\varepsilon_{\mathrm{SVD}}$, is chosen as 1.0×10^{-12}. The proposed eigenvalue solver converges when the column dimension of $\mathbf{X}$ reaches 12. The number of physically important eigenvalues found is 10.

Table VII lists the lowest three resonance frequencies as well as the backward errors of the proposed eigenvalue solution. The backward error measures the accuracy of both eigenvalues and eigenvectors, as can be seen from (43).

To simulate this example, the proposed eigenvalue solver only cost 1.3 s, whereas the state-of-the-art eigenvalue solver in Matlab used 200 Arnoldi steps, which cost 219 seconds, even though we provided $\mathrm{f}_0 = 6$ kGHz for Matlab to shift the eigenvalue spectrum. To simulate the same example, the number of Arnoldi steps required by the eigenvalue solver in [9] is 1000. The number of Arnoldi steps of [9] is different from that of Matlab's solver because the finite element matrix is formulated in a different way in [9]. Due to the linear complexity at each Arnoldi step, the total time cost by the solver in [9] is 1.9 s, which is less than Matlab's solver. As mentioned in the introduction part, the disadvantage of an Arnoldi-based eigenvalue solver is that there is no systematic

way to control the convergence of an Arnoldi iteration. The 200 used in Matlab and the 1000 used by the solver in [9] are both empirically adjusted in order to find the eigenvalues of interest. This problem is especially critical when dealing with a quadratic eigenvalue problem, the eigen-solutions of which are complex-valued. The number of Arnoldi iteration steps, and hence the Krylov-subspace vectors, required to find k physically important eigenvalues by the solver in [9] and that in Matlab is unknown and also can be large due to the limitation of an Arnoldi based eigenvalue solver, whereas the number of vectors required by the proposed solver is quantitatively controlled by checking the saturation of the rank of (9) or (32), and also small. In this example, the number of vectors required by the proposed eigenvalue solver is only 12 as compared to 200 used in Matlab and 1000 used in [9].

VI. Conclusion

The solution to eigenvalue problems is of great importance to electromagnetic analysis. In this paper, a deterministic-solution based fast eigenvalue solver is developed to find a complete set of eigenvalues and eigenvectors that are physically important for an arbitrary given frequency band. Let the number of such a complete set of eigenvalues be k, the proposed eigenvalue solver only needs to solve an eigenvalue problem of $O(k)$ to find the k eigenvalues and their corresponding eigenvectors. Such a reduced eigenvalue problem is orders of magnitude smaller than the original eigenvalue problem of $O(N)$. Furthermore, the $O(k)$ eigenvalue problem is built from $O(k)$ solutions to a deterministic problem, and hence existing methods for solving deterministic problems and their fast solvers can all be readily used to solve eigenvalue problems.

Both fast generalized eigenvalue solver and quadratic eigenvalue solver are developed. They are applicable to arbitrary 3-D structures and inhomogeneous materials. Both dielectrics and conductors can be lossy. Numerical experiments from microwave cavities to package structures to on-chip integrated circuits have demonstrated the accuracy, efficiency, and guaranteed convergence of the proposed deterministic-solution based fast eigenvalue solvers.

References

[1] A. Preumont, *Vibration Control of Active Structures: An Introduction*, 2nd ed. Amsterdam, The Netherlands: Kluwer, 2002, pp. 18–19.

[2] J. R. Brauer and G. C. Lizalek, "Microwave filter analysis using a new 3-D finite-element modal frequency method," *IEEE Trans. Microw. Theory Tech.*, vol. 45, no. 5, pp. 810–818, May 1997.

[3] J. Zhu and D. Jiao, "A theoretically rigorous full-wave finite-element-based solution of Maxwell's equations from DC to high frequencies," *IEEE Trans. Adv. Packag.*, vol. 33, no. 4, pp. 1043–1050, Nov. 2010.

[4] F. Sheng and D. Jiao, "A bandwidth unlimited fast frequency sweep algorithm for electromagnetic analysis," in *Proc. IEEE Int. Symp. Antennas Propag.*, Spokane, WA, Jul. 2011, p. 4.

[5] L. N. Trefethen and D. III Bau, *Numerical Linear Algebra*. Philadelphia, PA, USA: SIAM, 1997, pp. 179–250.

[6] ARPACK Houston, TX, 2008 [Online]. Available: http://www.caam.rice.edu/software/ARPACK/, Rice Univ.

[7] J. Lee, V. Balakrishnan, C.-K. Koh, and D. Jiao, "A linear-time complex-valued eigenvalue solver for electromagnetic analysis of large-scale on-chip interconnect structures," *IEEE Trans. Microw. Theory Tech.*, vol. 57, no. 8, pp. 2021–2029, Aug. 2009.

[8] J. Lee, V. Balakrishnan, C.-K. Koh, and D. Jiao, "From $O(k^2N)$ to $O(N)$: A fast complex-valued eigenvalue solver for large-scale on-chip interconnect analysis," *IEEE Trans. Microw. Theory Tech.*, vol. 57, no. 12, pp. 3219–3228, Dec. 2009.

[9] J. Lee, D. Chen, V. Balakrishnan, C.-K. Koh, and D. Jiao, "A quadratic eigenvalue solver of linear complexity for 3-D electromagnetics-based analysis of large-scale integrated circuits," *IEEE Trans. Comput.-Aided Design Integr. Circuits Syst.*, vol. 31, no. 3, pp. 380–390, Mar. 2012.

[10] L. Jaschke, *Preconditioned Arnoldi Methods for Systems of Nonlinear Equations*. Stuttgart, Germany: WiKu, 2004.

[11] Z. Jia, "The refined harmonic Arnoldi method and an implicitly restarted refined algorithm for computing interior eigenpairs of large matrices," *Appl. Numer. Math.*, vol. 42, pp. 489–512, 2002.

[12] K. Dookhitram, R. Boojhawon, and M. Bhuruth, "A new method for accelerating Arnoldi algorithms for large scale eigenproblems," *Math. Comput. Simulat.*, vol. 80, pp. 387–401, 2009.

[13] H. Wu and A. C. Cangellaris, "Model-order reduction of finite-element approximations of passive electromagnetic devices including lumped electrical-circuit models," *IEEE Trans. Microw. Theory Tech.*, vol. 52, no. 9, pp. 2305–2313, Sep. 2004.

[14] T. Wittig, R. Schuhmann, and T. Weiland, "Model order reduction for large systems in computational electromagnetics," *Linear Algebra Appl.*, vol. 415, no. 2, pp. 499–530, 2006.

[15] A. Schultschik *et al.*, "An adaptive multi-point fast frequency sweep for large-scale finite element models," *IEEE Trans. Magn.*, vol. 45, no. 3, pp. 1108–1111, Mar. 2009.

[16] F. Tisseur and K. Meerbergen, "The quadratic eigenvalue problem," *SIAM Rev.*, vol. 43, no. 2, pp. 235–286, 2001.

[17] H. Fang, W. Lin, and P. V. Dooren, "Normwise scaling of second order polynomial matrices," *SIAM J. Matrix Anal. Appl.*, vol. 26, no. 1, pp. 252–256, Sep. 2004.

[18] N. J. Higham, D. S. Mackey, F. Tisseur, and S. D. Garvey, "Scaling, sensitivity and stablility in the numerical solution of quadratic eigenvalue problems," *Int. J. Numer. Methods Eng.*, vol. 73, no. 3, pp. 344–360, Jan. 2008.

[19] J. Lee, T. Xiao, and Q. H. Liu, "A 3-D spectral-element method using mixed-order curl conforming vector basis functions for electromagnetic fields," *IEEE Trans. Microw. Theory Tech.*, vol. 54, no. 1, pp. 437–444, Jan. 2006.

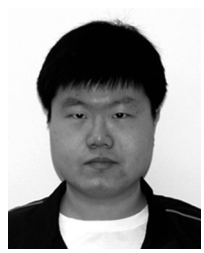

Feng Sheng received the B.S. degree in electronic and information engineering from Zhejiang University, Hangzhou, China, in 2006, and the Ph.D. degree from the School of Electrical and Computer Engineering at Purdue University, West Lafayette, IN, USA, in 2012.

He joined ANSYS Inc. in 2012. His current research interests include computational electromagnetics and the analysis and design of large-scale high-frequency integrated circuits.

Dan Jiao (S'00–M'02–SM'06) received the Ph.D. degree in electrical engineering from the University of Illinois at Urbana-Champaign, Urbana, IL, USA, in 2001.

She then worked at the Technology Computer-Aided Design (CAD) Division, Intel Corporation, until September 2005, as a Senior CAD Engineer, Staff Engineer, and Senior Staff Engineer. In September 2005, she joined Purdue University, West Lafayette, IN, as an Assistant Professor with the School of Electrical and Computer Engineering, where she is now a Professor. She has authored two book chapters and over 170 papers in refereed journals and international conferences. Her current research interests include computational electromagnetics, high-frequency digital, analog, mixed-signal, and RF integrated circuit (IC) design and analysis, high-performance VLSI CAD, modeling of microscale and nanoscale circuits, applied electromagnetics, fast and high-capacity numerical methods, fast time-domain analysis, scattering and antenna analysis, RF, microwave, and millimeter-wave circuits, wireless communication, and bioelectromagnetics.

Dr. Jiao has served as the Reviewer for many IEEE Journals and conferences. She is an Associate Editor of the IEEE Transactions on Components, Packaging, and Manufacturing Technology. She was the recipient of the

2013 S. A. Schelkunoff Prize Paper Award of the IEEE Antennas and Propagation Society. She was among the 85 engineers selected throughout the nation for the National Academy of Engineering's 2011 US Frontiers of Engineering Symposium. She was the recipient of the 2010 Ruth and Joel Spira Outstanding Teaching Award, the 2008 National Science Foundation (NSF) CAREER Award, the 2006 Jack and Cathie Kozik Faculty Start up Award (which recognizes an outstanding new faculty member of the School of Electrical and Computer Engineering, Purdue University), a 2006 Office of Naval Research (ONR) Award under the Young Investigator Program, the 2004 Best Paper Award presented at the Intel Corporation's annual corporate-wide technology conference (Design and Test Technology Conference) for her work on generic broadband model of high-speed circuits, the 2003 Intel Corporation's Logic Technology Development (LTD) Divisional Achievement Award in recognition of her work on the industry-leading BroadSpice modeling/simulation capability for designing high-speed microprocessors, packages, and circuit boards, the Intel Corporation's Technology CAD Divisional Achievement Award for the development of innovative full-wave solvers for high frequency IC design, the 2002 Intel Corporation's Components Research the Intel Hero Award (Intel-wide she was the tenth recipient) for the timely and accurate 2-D and 3-D full-wave simulations, the Intel Corporation's LTD Team Quality Award for her outstanding contribution to the development of the measurement capability and simulation tools for high frequency on-chip crosstalk, and the 2000 Raj Mittra Outstanding Research Award presented by the University of Illinois at Urbana-Champaign.